Journal of Molecular Catalysis A: Chemical 309 (2009) 79–88

Contents lists available at ScienceDirect

Journal of Molecular Catalysis A: Chemical

journal homepage: www.elsevier.com/locate/molcata

# Relation between sulfur coordination of active sites and HDS activity for Mo and NiMo catalysts

Bas M. Vogelaar[a,*], Narinobu Kagami[b], Thomas F. van der Zijden[a], A. Dick van Langeveld[a], Sonja Eijsbouts[c], Jacob A. Moulijn[a]

[a] Delft University of Technology, Faculty of Applied Sciences, Department of Reactor and Catalysis Engineering, Julianalaan 136, 2628 BL Delft, The Netherlands
[b] Idemitzu Kosan Co. Ltd., 26 Anesakikaigan Ichihara-city, Chiba 229-0107, Japan
[c] Albemarle Catalysts, P.O. Box 37650, 1030 BE Amsterdam, The Netherlands

ARTICLE INFO

*Article history:*
Received 13 December 2008
Received in revised form 21 April 2009
Accepted 25 April 2009
Available online 3 May 2009

*Keywords:*
Hydrodesulfurization
Molybdenum sulfide
Active phase
CO adsorption
Infrared spectroscopy

ABSTRACT

The structure of sulfidic Type I and Type II Mo and NiMo alumina supported hydrodesulfurization (HDS) catalysts was studied using infrared (IR) analysis of adsorbed CO. The results were compared to the catalytic activity in gas phase thiophene and liquid phase dibenzothiophene HDS reactions. IR analysis confirmed the presence of $MoS_2$- and NiMoS-type phases. The Type II NiMo catalyst (prepared using NTA as chelating agent) had a fully promoted edge structure, whereas the Type I (calcined) NiMo catalyst exhibited both promoted and unpromoted edge sites, confirming that NTA enhances the Ni-decoration of the $MoS_2$ edges. The active phase in both types of catalysts exhibited a dynamic and reversible behavior in terms of sulfur coordination. The catalysts exposed a higher number and/or a higher degree of coordinative unsaturation of vacant sites under gas phase thiophene HDS conditions than directly after sulfidation. The NiMo catalysts could be fully restored to their initial state by resulfiding after thiophene HDS, whereas some sites of the Mo catalysts were irreversibly blocked. Apparently, the NiMo catalysts were able to suppress coke deposition on the active sites under the conditions applied, in contrast to the Mo catalysts. An inverse correlation was found between the gas phase thiophene HDS conversion and the number of vacant sites present on the catalyst surface. A similar trend was observed for the ratio between hydrogenation and direct desulfurization of dibenzothiophene in the liquid phase HDS reaction. These correlations show that the thiophene HDS reaction and the dibenzothiophene hydrogenation pathway are catalyzed by sulfided species on the active phase, while the direct desulfurization pathway is catalyzed by vacant sites.



## 1. Introduction

CoMo and NiMo based hydrodesulfurization (HDS) catalysts have been used in industrial hydrotreating processes for decades [1]. Although many improvements have been made in the composition, metal dispersion and support material of these catalysts, their formulation has basically remained unchanged. In order to further improve these catalysts, fundamental insights in the structure of these catalysts and the nature of the active sites are needed. Although great progress has been made over the years, crucial details regarding the structure of this type of catalysts on the atomic scale have not been fully uncovered. The observation of unpromoted and promoted $MoS_2$ slabs under the STM microscope [2,3] inspired several research groups to perform new modeling studies on the edge structure of $MoS_2$ slabs in HDS catalysts, see e.g. [4–6]. Comprehensive reviews on this topic were published by Raybaud [7] and Sun et al. [8]. An example of different edge configurations for a $MoS_2$ slab is shown in Fig. 1. The coordination number or degree of coordinative unsaturation of the edge Mo atoms changes as a function of sulfur content [3]. Sulfur atoms on the edges of the active phase can be removed by reacting with hydrogen, yielding coordinatively unsaturated (cus) Mo sites. The case of promoted HDS catalysts is more complex [9]. Most researchers have accepted the CoMoS/NiMoS model, in which the promoter atoms are atomically dispersed over the $MoS_2$ edges, forming the so-called CoMoS or NiMoS phase. In this model the promoter atoms are either the active centers or able to enhance (promote) the activity of the $MoS_2$ edge sites [1]. It has been well established that at least two different types of active sites are involved in HDS reactions and it is generally believed that vacant (cus) sites are responsible for the removal of hetero-atoms [1]. Furthermore, several researchers propose that fully sulfided species (i.e. sulfur that is a part of the catalyst active phase) may play a role in the HDS reaction [10–13]. These sugges-

* Corresponding author. Current address: Albemarle Catalysts, P.O. Box 37650, 1030 BE Amsterdam, The Netherlands. Tel.: +31 20 6347648; fax: +31 20 6347653.
*E-mail address:* Bas.Vogelaar@albemarle.com (B.M. Vogelaar).

1381-1169/$ – see front matter © 2009 Elsevier B.V. All rights reserved.
doi:10.1016/j.molcata.2009.04.018

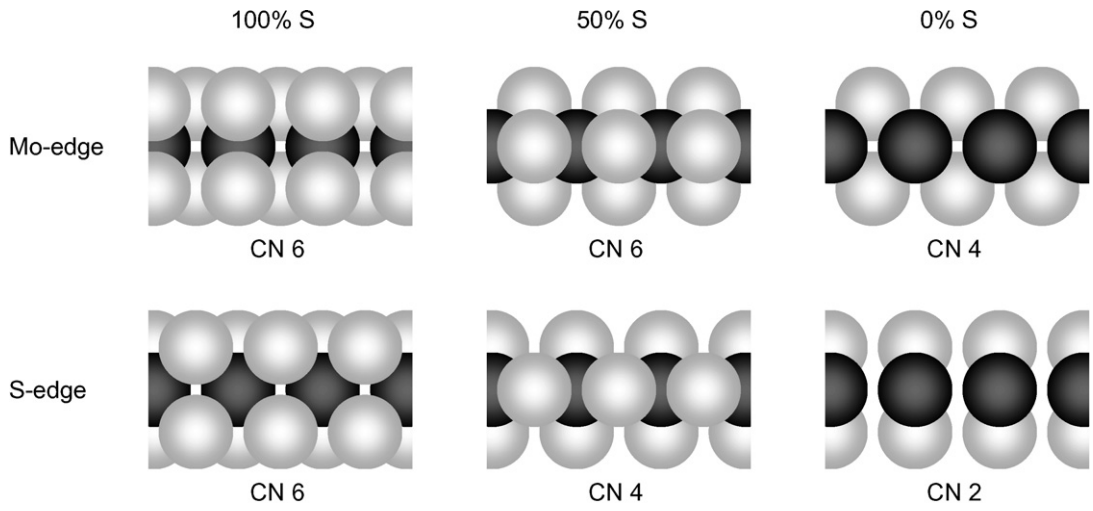


**Fig. 1.** Ball model (side view) of the edges of a $MoS_2$ slab at different sulfur loadings, adapted from Ref. [3]. Dark spheres represent Mo, light spheres S atoms. Indicated are the total sulfur coordination (%) of the edge and the coordination number (CN) for Mo in each case.

tions are mostly based on the observed selectivity of the catalyst, which was recently reported again for the HDS of dibenzothiophene [14].

In the present study, the active phase of Mo and NiMo based HDS catalysts was characterized using infrared (IR) analysis of adsorbed CO. Furthermore, these results were correlated to the thiophene and dibenzothiophene HDS activity of the different catalysts. The adsorption of probe molecules like CO, coupled with vibrational spectroscopy is a widely used and powerful tool for the identification of the surface structure and properties of various inorganic materials, including HDS catalysts [15–17]. Adsorbed CO molecules interact with transition metals through their molecular orbitals, which affects the CO bond strength. The resulting CO bond stretching frequency observed in the IR spectrum is a function of the type of metal on which it adsorbs, the oxidation state of the metal and the coordination number of the metal center. For this study, Mo and NiMo based catalysts were used with different morphologies (so-called Type I and Type II). It is generally believed that the Type II active phase has improved properties, resulting in a higher HDS activity (e.g. see [18–20]). Dried Type II catalysts were prepared using nitrilo triacetic acid (NTA) as a complexing agent and calcined Type I catalysts were prepared without NTA. The catalysts were subjected to various treatments including HDS reactions, in order to gain further insight in the active phase structure and its catalytic function.

## 2. Experimental

### 2.1. Catalysts

Four different catalysts were prepared, as summarized in Table 1. A solution of ammonium dimolybdate $(NH_4)_2Mo_2O_7$ and nickel nitrate $Ni(NO_3)_2$ was impregnated onto 1.5 mm cylindrical extrudates of a high purity $\gamma$-$Al_2O_3$ support (Ketjen CK 300). The resulting catalysts were dried at 393 K for 1 h and calcined at 723 K for 1 h (heating rate 5 K/min). This procedure leads to the formation of typical Type I HDS catalysts. Their so-called Type II counterparts were prepared using a different procedure. Nitrilo triacetic acid (NTA) was added to the impregnating solution as a chelating agent, with a ratio of 1.2 mol NTA per mol Mo (i.e. 2.4 mol NTA per mol Ni). The resulting catalysts were dried at 393 K for 1 h and not calcined. Note that for measuring the catalyst properties (Table 1), all catalysts were calcined. After preparation, the catalyst extrudates were crushed and sieved to obtain a particle fraction of 75–125 μm diameter for the activity tests and a fraction <75 μm diameter for the IR analyses. The following gas phase sulfiding procedure was used: the catalyst was exposed to a mixture of 5 vol% $H_2S$ and 50 vol% $H_2$ in Ar. The temperature was held at 298 K for 0.5 h, increased with 10 K/min to 673 K and held for 2 h at 673 K. A lower heating rate of 2 K/min was applied for the sulfiding of the NTA based catalysts, to ensure the homogeneous decomposition of the chelating agent. Throughout this work, Type I catalysts are indicated as Mo and NiMo, while Type II catalysts are indicated as Mo(NTA) and NiMo(NTA).

### 2.2. IR analysis of adsorbed CO

A dedicated infrared in situ analysis setup (IRIS) was used for this study, as described in [20]. About 20 mg of the crushed catalyst (<75 μm) was pressed into a self-supporting disk by applying a pressure of 0.5 GPa for 1 min. The NiMo catalysts were diluted with an equal weight of the $\gamma$-$Al_2O_3$ support material, before pressing, to enhance the transparency of the samples. Inside the IRIS equipment, the sample could be transported between the "high temperature chamber" (HTC) for pretreatment and the "infrared chamber" (IRC) for analysis, without exposure to air. Several pretreatment procedures were carried out; sulfiding (using the procedure described in Section 2.1), treatment in $H_2$ and thiophene HDS in a mixture of 4.3 vol% thiophene in $H_2$. During pretreatment in the HTC, the sample was subjected to a gas stream of

**Table 1**
Properties of the prepared catalysts.

| Catalyst | Mo loading (wt% $MoO_3$) | Ni loading (wt% NiO) | Pore volume ($cm^3/g$) | Surface area ($m^2/g$) |
|---|---|---|---|---|
| Mo | 10.25 | – | 0.58 | 274 |
| Mo(NTA) | 10.12 | – | 0.58 | 272 |
| NiMo | 10.04 | 2.44 | 0.56 | 268 |
| NiMo(NTA) | 9.93 | 2.37 | 0.56 | 265 |

Analysis data were provided by Albemarle Catalysts. Catalyst properties were measured after calcination.

60 ml/min at 170 kPa absolute pressure, at a temperature of 673 K, for 2 h by default unless stated otherwise. The thiophene mixture was obtained by flowing $H_2$ through a saturator containing liquid thiophene at 283 K. After each treatment, the HTC was purged with 200 ml/min He while cooling down to room temperature and evacuated overnight using a turbomolecular drag pump. The IR analysis was performed after moving the sample down into the IRC and cooling to 140 K, using liquid nitrogen. CO was admitted to the chamber at increasing pressures of 10, 50, 100, 250, 500 and 750 Pa. IR transmission spectra were taken using a Nicolet Magna-IR 550 spectrometer. The contribution of the gas phase inside and outside the cell was eliminated by moving the sample out of the IR beam and taking a background spectrum at each pressure. Before CO admission, a single spectrum was recorded for baseline correction and to visualize the spectral features of the catalyst itself (e.g. deposited carbonaceous species). After analysis, the adsorbed CO was removed by heating the IRC to room temperature at 10 K/min under continuous evacuation by the turbomolecular drag pump. The system was then re-pressurized with He and the sample was transported back to the HTC for further treatment or replacement by a new sample. This way, cyclic tests were performed, in which consecutive treatments were carried out on the same sample.

### 2.3. HDS activity measurements

The thiophene HDS conversion was measured in an atmospheric fixed bed reactor system at 673 K. A fixed weight of catalyst was loaded into the reactor; 500 mg for the Mo based catalyst and 100 mg for the NiMo based catalysts. The catalyst particles (75–125 μm) were diluted with an equal volume of SiC particles to optimize heat transfer in the packed bed. The catalysts were presulfided in situ using the standard procedure (described in Section 2.1). In selected cases, the catalyst was treated in 10 vol% $H_2S$ in Ar during 2 h after presulfiding, in order to achieve a maximum degree of sulfur coordination. Directly after pretreatment, the gas flow was switched to the reaction mixture containing 4.3 vol.% thiophene in balance $H_2$ and the catalytic conversion was determined by analyzing the outlet gas stream using an on-line gas chromatograph during the first 4 h on stream.

The dibenzothiophene HDS measurements were performed in a high pressure 200 ml swinging-capillary autoclave reactor. Experiments were only performed on the NiMo (Type I) catalyst, because the main objective of this part of the work was to assess the effect of sulfur coordination on catalytic selectivity. In each experiment, 200 mg of crushed catalyst was placed on a tray in a separate pretreatment cell for gas phase presulfiding or $H_2$ treatment at atmospheric pressure, connected to the autoclave vessel via a ball valve. Sulfiding was carried out using the standard procedure described in Section 2.1. In one experiment, the catalyst was subsequently exposed to a 60 ml/min $H_2$ stream during 4 h at 673 K. After pretreatment, the catalyst was directly immersed into the reaction mixture by rotating the tray, avoiding thus the exposure of the pretreated catalyst to air. The reaction liquid consisted of 0.2 wt% dibenzothiophene (DBT) and 0.2 wt% octadecane (n-$C_{18}$) as internal standard in hexadecane (n-$C_{16}$). The system was purged with $H_2$, rapidly heated to the reaction temperature of 623 K and pressurized with $H_2$ to 5 MPa. Samples from the reaction liquid were taken at regular intervals and the resulting pressure loss was compensated by adding $H_2$. The liquid sample volume was small (about 1 ml), therefore not affecting the liquid concentration significantly. The reaction products were analyzed using a gas chromatograph with FID detector.

### 2.4. IR analysis after liquid phase HDS

The NiMo (Type I) catalyst was analyzed in the IRIS setup after exposure to liquid phase DBT HDS reaction conditions using the following procedure. First, the IRIS sample holder, containing the NiMo sample, was mounted inside the autoclave reactor. Then, the sample was sulfided using the standard procedure and immersed in the reaction liquid to undergo the DBT HDS reaction for 4 h. After cooling down the reactor, the sample was rinsed with toluene (Acros, >98% purity) at room temperature to remove residues of the reaction mixture. The sample was then immediately transferred to the IRIS, which was purged with helium. The remaining toluene was removed from the sample by heating it at 383 K for 2 h under a helium flow of 200 ml/min, followed by evacuation overnight at the same temperature. Using

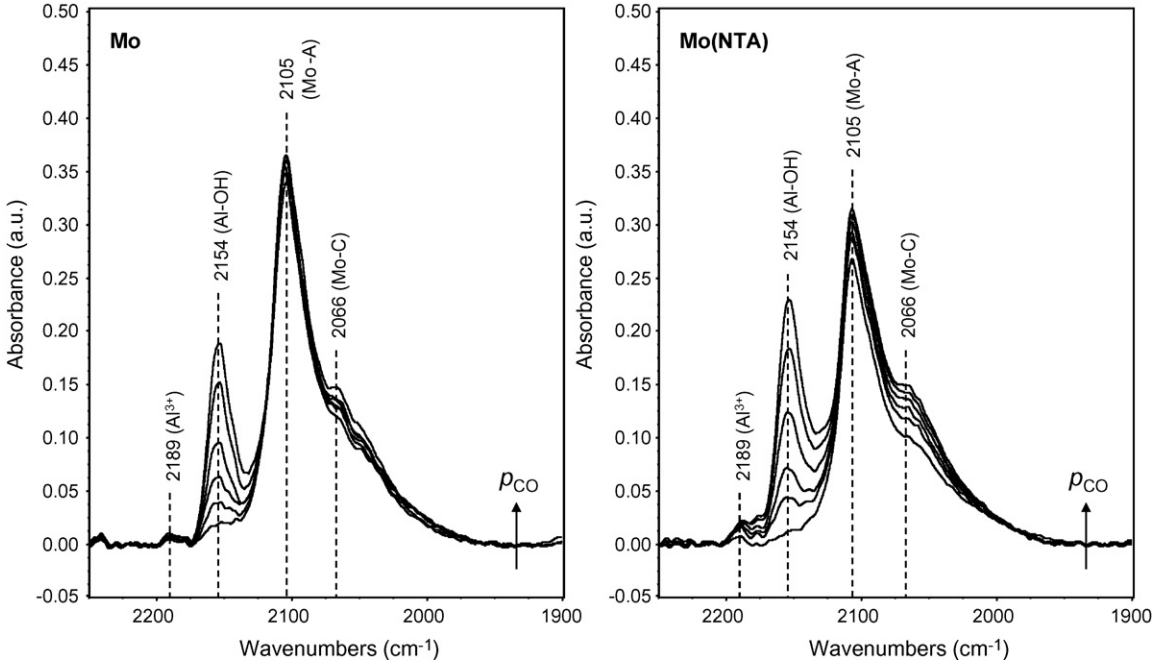


**Fig. 2.** IR spectra of CO adsorbed at increasing pressure on Mo and Mo(NTA) catalysts after sulfiding and treatment in $H_2$ for 0.5 h.

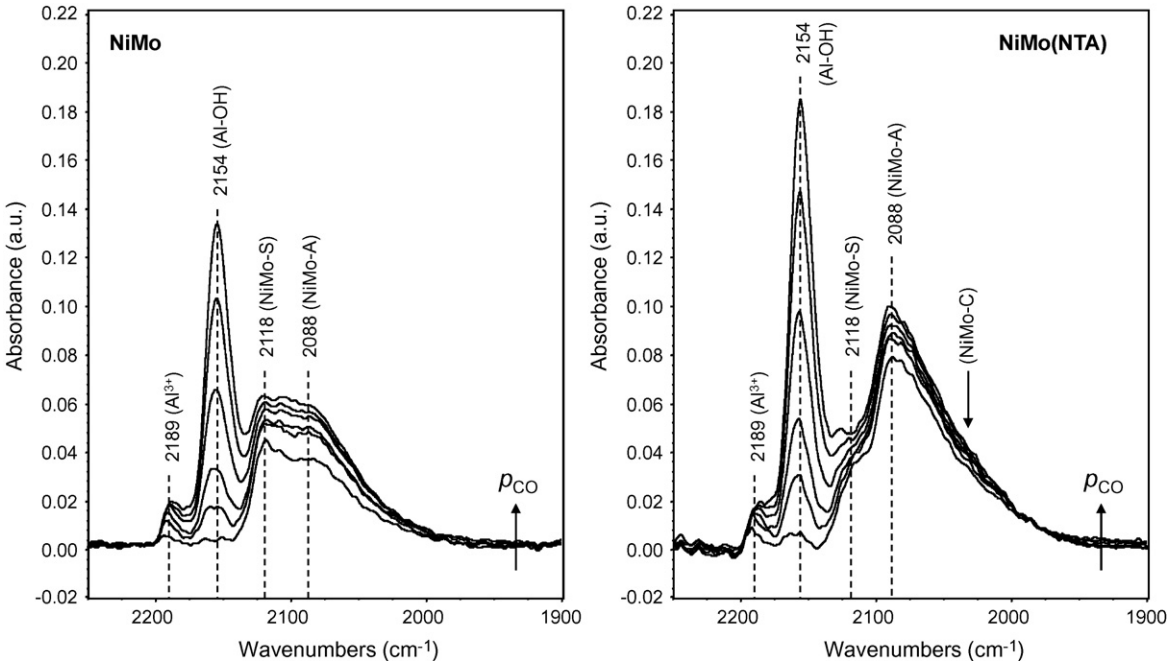


**Fig. 3.** IR spectra of CO adsorbed at increasing pressure on NiMo and NiMo(NTA) catalysts after sulfiding and treatment in $H_2$ for 0.5 h.

this procedure, the exposure of the sample to air was kept to a minimum.

## 3. Results

### 3.1. Infrared analysis

The resulting IR spectra of CO adsorbed on the catalysts after sulfiding and treatment in $H_2$ for 0.5 h at 673 K are shown in Figs. 2 and 3. To help the reader, the different peak positions have already been labeled according to the corresponding active phase type (Mo or NiMo) and the type of adsorption site (S, A, B or C), throughout Section 3 and in the figures. The assignment of these peaks will be described in Section 4; see also Tables 2 and 3. In all spectra, two features can be observed, which increase strongly with the CO pressure. A weak band is observed at 2189 $cm^{-1}$ ($Al^{3+}$ sites) and a strong band at 2154 $cm^{-1}$ (Al–OH sites). These features are attributed to the support material [21] and overlap the other bands partially at high CO pressure. The other bands are different for the Mo and NiMo catalysts and are already saturated at very low CO pressures (50 Pa). These typical features are attributed to CO adsorbed on the active phase of the catalysts [21] and are labeled according to Table 3. Only the spectra of CO adsorbed at 10 Pa pressure are shown in the next figures because the features of the active phase could be obscured by the bands of CO adsorbed on the support at higher CO pressures.

The spectra of both types of catalysts (Mo and NiMo) strongly depend on the pretreatment conditions (Fig. 4). The freshly sulfided Mo (Type I) catalyst closely resembles the $H_2$ treated catalyst (Fig. 4a and b), although the CO adsorption increases after $H_2$ exposure. Two hours of thiophene HDS yield the opposite effect (Fig. 4c). The CO adsorption decreases drastically and a new feature is observed around 2090 $cm^{-1}$ (Mo–B sites). The NiMo catalyst exhibits a different behavior. After sulfiding (Fig. 4a) and $H_2$ treatment (Fig. 4b), the CO adsorption bands are low. However, a very strong band is observed at 2077 $cm^{-1}$ after thiophene HDS (NiMo–B sites, Fig. 4c) and this band does not decrease significantly even after 4 h of thiophene exposure (Fig. 4d).

The IR spectra from the cyclic test with the Mo catalyst are shown in Fig. 5. Clearly, a prolonged $H_2$ treatment of 4 h directly after the sulfidation step (Fig. 5a) leads to a strong increase in the IR band intensity for adsorbed CO (Fig. 5b). These bands drastically decrease after a consecutive thiophene treatment while the peak at 2090 $cm^{-1}$ (Mo–B sites) remains as most prominent contribution (Fig. 5c). The resulfidation treatment, directly following the thiophene exposure, restores the band at 2105 $cm^{-1}$ (Mo–A sites) as the largest contributor to the CO spectrum (Fig. 5d). The resulting spectrum is similar to that of the freshly sulfided catalyst (Fig. 5a).

**Table 2**
IR band positions of CO adsorbed on Mo, Ni and support centers, taken from the literature data.

| Species | Wavenumber range | Reference |
|---|---|---|
| $Al^{3+}$ | 2189 $cm^{-1}$ | [26] |
| Al–OH | 2154 $cm^{-1}$ | [26] |
| $Mo^{4+}$ | 2195–2160 $cm^{-1}$ | [27] |
| $Mo^{\phi+}$ ($2<\phi<4$) | 2100–2080 $cm^{-1}$ | [27] |
| $Mo^{2+}$ | 2070–2050 $cm^{-1}$ | [27] |
| $Mo^{\delta+}$ ($0<\delta<2$) | 2055–2015 $cm^{-1}$ | [27] |
| $Mo^{0}$ | 2045–2025 $cm^{-1}$ | [27] |
| $Ni^{2+}$ | 2210–2170 $cm^{-1}$ | [28] |
| $Ni^{\delta+}$ ($0<\delta<2$) | 2120–2080 $cm^{-1}$ | [28] |
| $Ni^{0}$ | 2060–2020 $cm^{-1}$ | [28] |

**Table 3**
Description of CO adsorption sites on $MoS_2$ and NiMoS type catalysts according to this study.

| Label | Sulfur coordination | IR band position | Species[a] |
|---|---|---|---|
| Mo-S | Highest | Not observed | $Mo^{4+}$ |
| Mo-A | High | 2105 $cm^{-1}$ | $Mo^{\phi+}$ ($2<\phi<4$) |
| Mo-B | Low | 2090 $cm^{-1}$ | $Mo^{\phi+}$ ($2<\phi<4$) |
| Mo-C | Lowest | Shoulder at 2066 and 2045 $cm^{-1}$ | $Mo^{\delta+}$ ($0<\delta<2$) |
| NiMo-S | Highest | 2118 $cm^{-1}$ | $Ni^{\delta+}$ ($0<\delta<2$) |
| NiMo-A | High | 2088 $cm^{-1}$ | $Ni^{\delta+}$ ($0<\delta<2$) |
| NiMo-B | Low | 2077 $cm^{-1}$ | $Ni^{\delta+}$ ($0<\delta<2$) |
| NiMo-C | Lowest | Shoulder around 2050 $cm^{-1}$ | $Ni^{0}$ |

[a] According to Table 2.

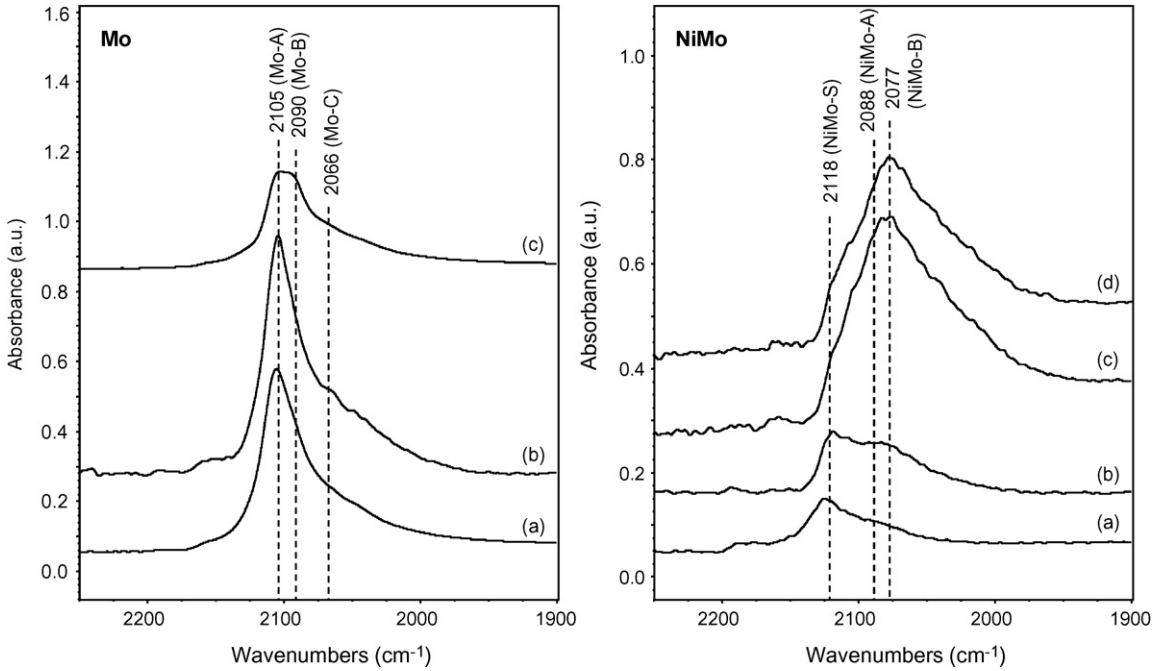


**Fig. 4.** IR spectra of CO adsorbed on Mo and NiMo catalysts after (a) sulfiding, (b) sulfiding and 0.5 h $H_2$ treatment, (c) sulfiding and 2 h thiophene HDS and (d) sulfiding and 4 h thiophene HDS.

However, the shoulder around 2045 $cm^{-1}$ (Mo–C sites) has about the same intensity as directly after sulfiding and is therefore more pronounced in this spectrum. The other spectra in Fig. 5 show the IR bands in the carbon bond-stretching region. Two bands evolve at 1467 and 1573 $cm^{-1}$ upon thiophene exposure, indicating carbonaceous deposits on the catalyst (Fig. 5c). As the nature of these carbonaceous species is not clear, they will be referred to as "coke". The consecutive resulfiding step reduces the coke bands somewhat but not fully to the level of the freshly sulfided catalyst. The other features appear to have no direct correlation with the pretreatment conditions.

CO adsorption after sulfiding is very low in the cyclic test on the NiMo catalyst (Fig. 6). A similar spectrum is observed after 4 h of $H_2$ treatment (Fig. 6b) as after 0.5 h of $H_2$ (Fig. 4c), although the band at 2077 $cm^{-1}$ (NiMo–B sites) is higher in intensity. The shape of the spectrum is the same following exposure to thiophene for 4 h, only its intensity is slightly higher and a shoulder can be distinguished around 2105 $cm^{-1}$ (Mo–A sites, Fig. 6c). Resulfiding (Fig. 6d) yields a spectrum similar to the one directly after sulfiding (Fig. 4b), while a consecutive treatment in $H_2$ (Fig. 6e) results in a spectrum that is virtually identical to the one after the first $H_2$ treatment (Fig. 6b). The bands in the coke region clearly increase after thiophene expo-

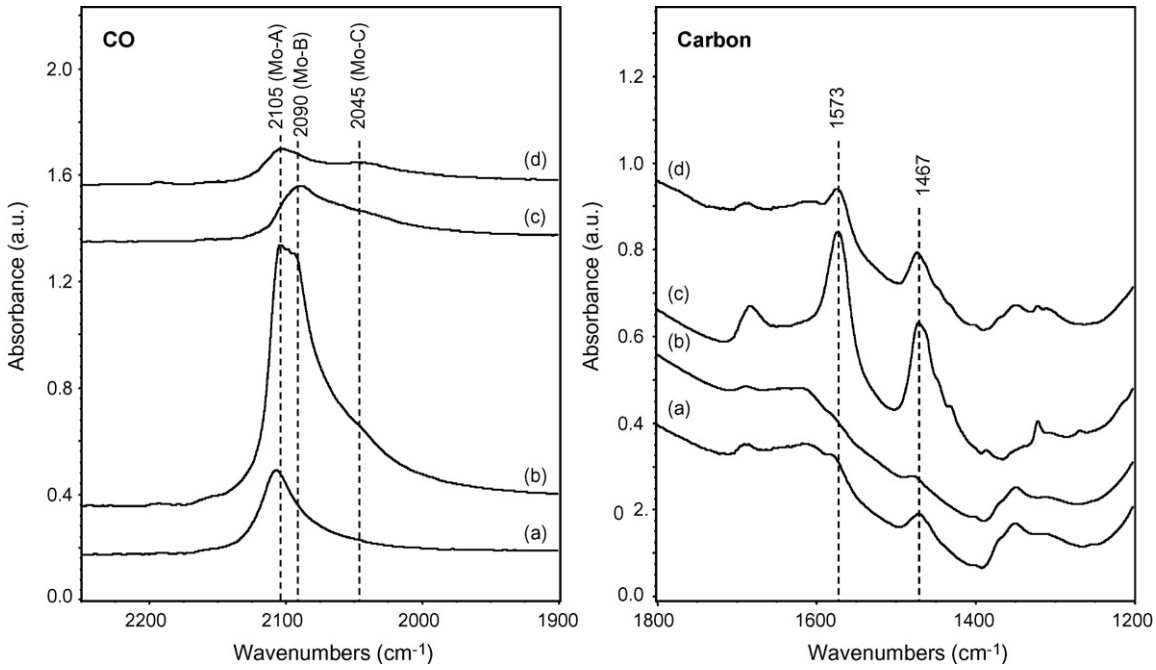


**Fig. 5.** Cyclic test of the Mo catalyst: IR spectra of CO and coke after (a) sulfiding, (b) 4 h $H_2$ treatment, (c) 4 h thiophene HDS and (d) resulfiding.

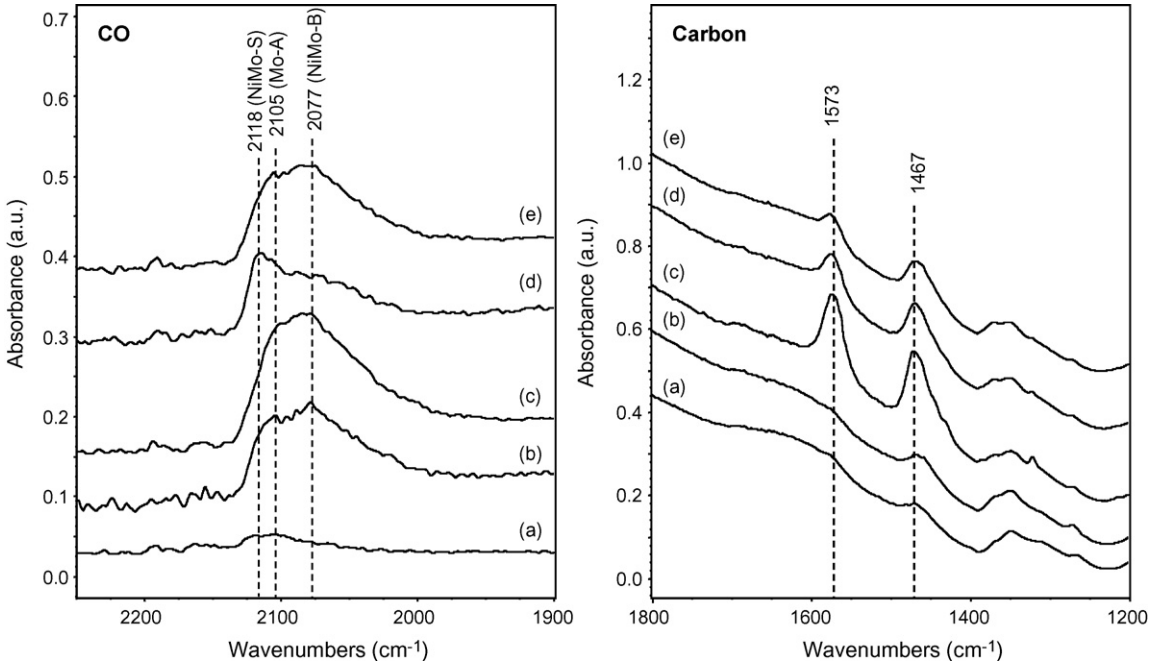


**Fig. 6.** Cyclic test of the NiMo catalyst: IR spectra of CO and coke after (a) sulfiding, (b) 4 h $H_2$ treatment, (c) 4 h thiophene HDS, (d) resulfiding and (e) 4 h $H_2$ treatment.

sure in this cyclic test, but they are significantly reduced after the consecutive $H_2$ treatment.

The cyclic test on the NiMo(NTA) catalyst (Fig. 7) produces spectra very similar to the NiMo catalyst, only the contribution at 2105 $cm^{-1}$ (Mo–A sites) is missing. The bands on the low-wavenumber side increase in intensity upon consecutive $H_2$ and thiophene treatment (Fig. 7b and c). Resulfiding produces a spectrum comparable to the freshly sulfided state, albeit that the band at 2118 $cm^{-1}$ (NiMo–S sites) is slightly lower (Fig. 7d). The bands in the coke region are most pronounced for the freshly sulfided catalyst (Fig. 7a), probably as a result of the decomposition of the organic chelating agent (NTA). The $H_2$ treatment strongly reduces these bands in intensity, but they increase again after the consecutive thiophene exposure. The resulfiding step produces the spectrum with the lowest contribution in the coke region (Fig. 7d).

The IR spectra of the NiMo catalyst exposed to liquid phase DBT HDS conditions are shown in Fig. 8. The CO adsorption spectrum, directly after DBT HDS (Fig. 8a), shows mainly a sharp peak at 2118 $cm^{-1}$ (NiMo–S sites). The band at 2077 $cm^{-1}$ (NiMo–B sites) increases upon subsequent $H_2$ treatment at 673 K (Fig. 8b) and decreases after a following sulfiding treatment (Fig. 8c). Finally, this band dominates the spectrum after exposing the same sample again to $H_2$ (Fig. 8d). The amount of carbonaceous species on the sample

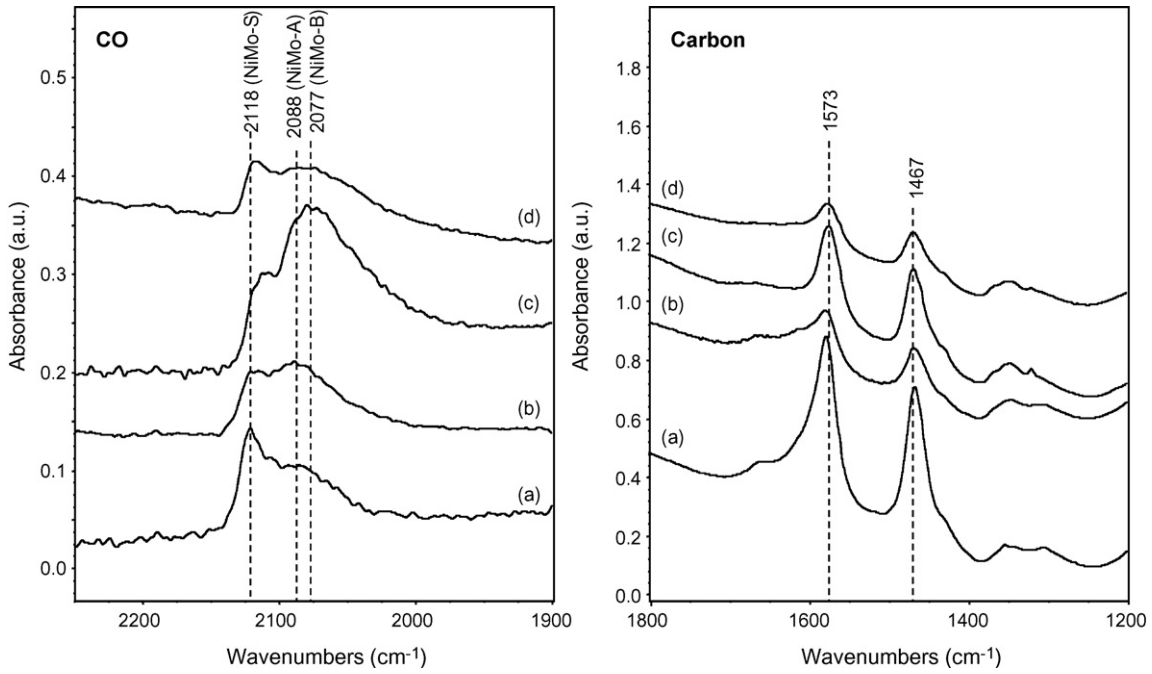


**Fig. 7.** Cyclic test of the NiMo(NTA) catalyst: IR spectra of CO and coke after (a) sulfiding, (b) 4 h $H_2$ treatment, (c) 4 h thiophene HDS and (d) resulfiding.

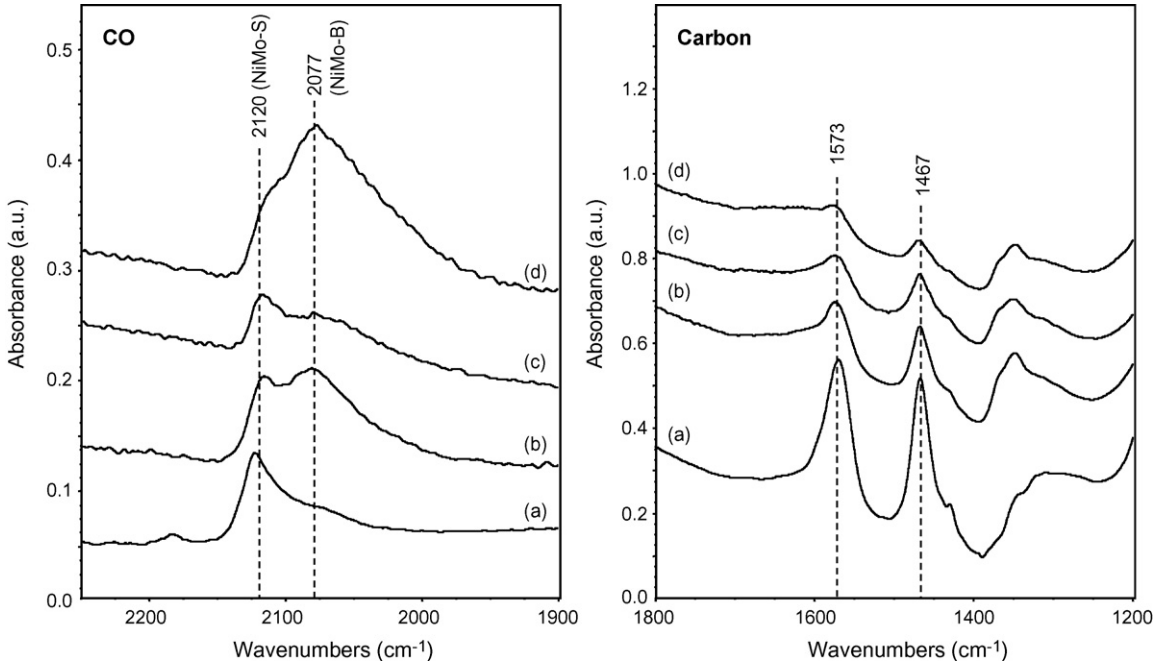


**Fig. 8.** IR spectra of CO and carbonaceous species on the NiMo catalyst after subsequent (a) DBT HDS, (b) $H_2$ treatment, (c) resulfiding and (d) another $H_2$ treatment.

is the highest directly after the liquid phase exposure and decreases after each subsequent gas phase treatment.

### 3.2. HDS activity measurements

The thiophene conversion of the catalysts is plotted as a function of time on stream during the first 4 h directly after presulfidation in Fig. 9. All four catalysts exhibit significant deactivation and the conversion approaches a steady state after 4 h. Pretreatment in $H_2S$/Ar (without $H_2$) after sulfidation results in a significantly higher initial conversion than the standard sulfiding procedure. This effect is most pronounced for the NiMo(NTA) catalyst.

The results of the liquid phase DBT HDS activity measurements are shown in Fig. 10. Total conversion is reached in 4 h for both catalysts; the NiMo (Type I) catalyst after sulfidation and the same catalyst after sulfidation and 4 h $H_2$ treatment. The observed reaction products are biphenyl (BPh) and cyclohexyl benzene (CHB). The ratio between these reaction products is shown as function of DBT conversion in Fig. 11. The $H_2$-pretreated catalyst shows a lower CHB/BPh ratio throughout the DBT conversion range.

## 4. Discussion

### 4.1. Effects of NTA

The band attributed to CO adsorbed on the support (Al–OH sites at 2154 $cm^{-1}$) has a higher intensity in the spectra of both NTA based catalysts than in the spectra of their calcined counterparts (Figs. 2 and 3; note that the figures are plotted on the same scale). This suggests that the active phase covers less support surface area in the case of the NTA catalysts and, because the support material and the metal loading are the same, the stacking degree of the $MoS_2$ slabs is higher (and the dispersion lower). This has already been reported for catalysts prepared using chelating agents, see e.g. Hensen et al. [18], and may also explain the noticeably lower thiophene conversion of the NTA catalysts in Fig. 9. Furthermore,

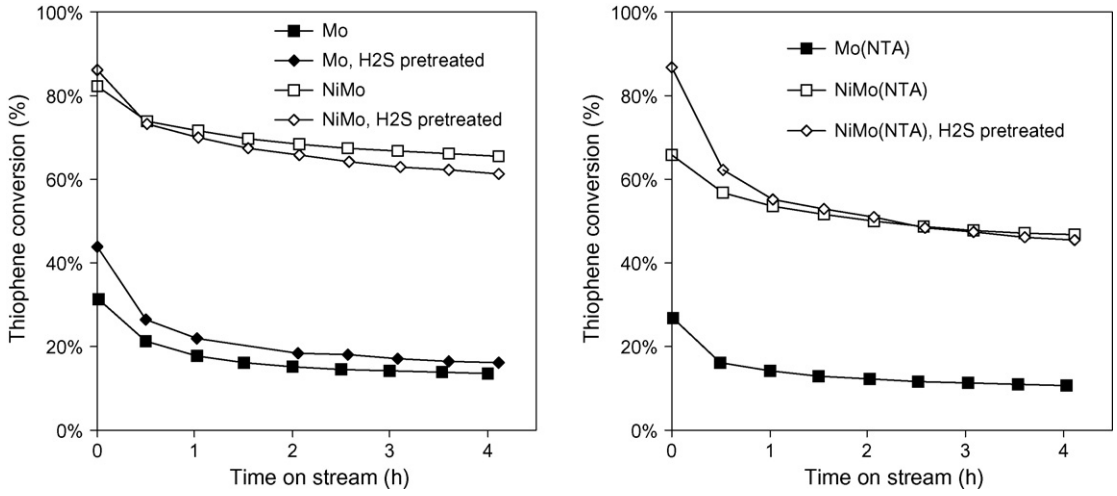


**Fig. 9.** Thiophene HDS conversion as function of time on stream in atmospheric flow reactor at 673 K; partially adapted from Ref. [10]. Note that the Mo catalysts were tested at a five times lower space velocity.

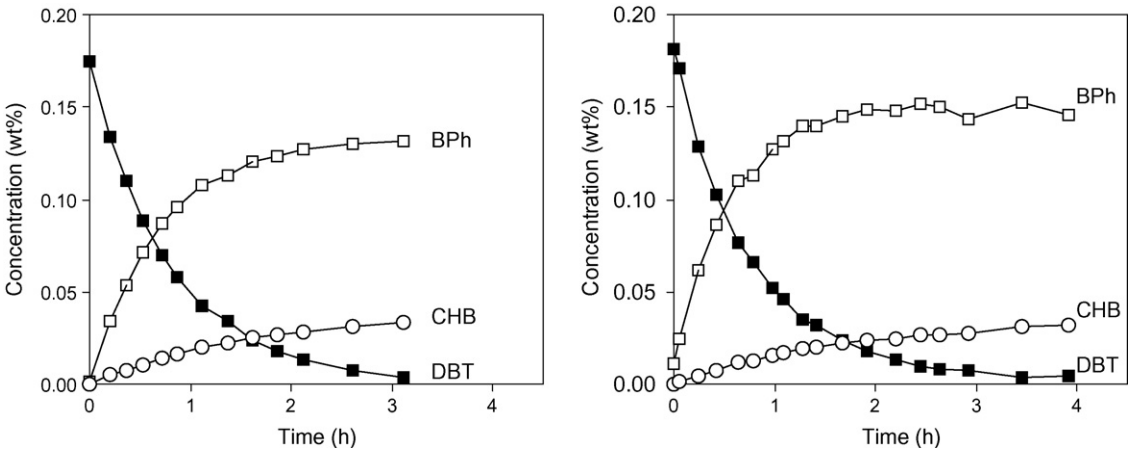


**Fig. 10.** Liquid phase DBT conversion in autoclave at 623 K and 5 MPa pressure, using the sulfided NiMo catalyst (left) and same after $H_2$ pretreatment (right).

the completely different spectra of NiMo(NTA) as compared to Mo demonstrate that a new phase is formed upon Ni promotion, in agreement with the CoMoS or NiMoS model. It is believed that a complexing agent improves the interaction between the promoter (Ni) and the $MoS_2$ slabs. This effect is thought to be due to the delayed sulfidation of the Ni–NTA complex, which leads to the more simultaneous sulfidation of Ni and Mo and results in an increased decoration of the $MoS_2$ edges by Ni atoms [19]. Interestingly, the NiMo catalyst shows features around 2105 $cm^{-1}$ (Mo–A sites), which is the dominant feature of the unpromoted catalysts (Fig. 2), whereas the NiMo(NTA) catalyst does not exhibit these features. This indicates that, indeed, the chelating agent helps to increase the Ni-decoration of the $MoS_2$ slabs. A similar effect was recently shown for CoMo catalysts by Lélias et al. [20].

### 4.2. Assignment of IR bands

Comprehensive IR studies of HDS catalysts using CO adsorption are not abundant; good references are publications by e.g. Maugé et al. [20–24], Van Langeveld et al. [25,26], and Wu et al. [27,28]. Table 2 gives an overview (adapted from [26–28]) of the spectral regions, in which IR bands of CO adsorbed (end-on) on Mo, Ni or support centers can be expected. The bands of the $Al_2O_3$ support are well documented and can easily be identified in Figs. 2 and 3. The spectral features attributed to the active metals in the present study are summarized in Table 3 and will be described in Sections 4.2.1 and 4.2.2.

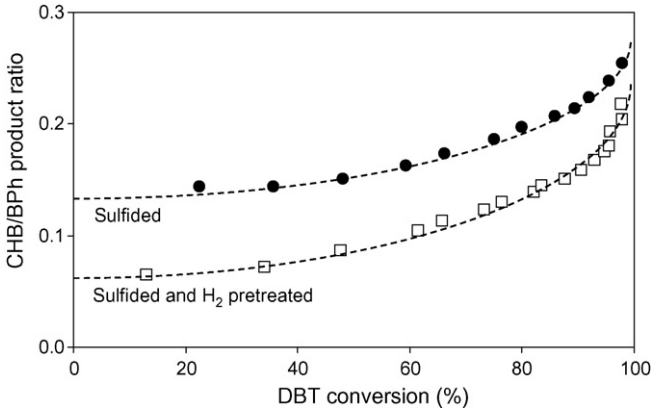


**Fig. 11.** HYD/DDS selectivity of the NiMo catalyst versus DBT conversion as function of catalyst pretreatment conditions.

#### 4.2.1. Unpromoted catalysts

The following features observed in Figs. 2, 4 and 5 can be attributed to CO adsorption on the unpromoted $MoS_2$ active phase (Table 2): a band at 2105 $cm^{-1}$ (Mo–A sites), a band at 2090 $cm^{-1}$ (Mo–B sites) and shoulders at 2066 $cm^{-1}$ and 2045 $cm^{-1}$ (Mo–C sites). The distinct peak at 2105 $cm^{-1}$ (Mo–A sites) in Figs. 2 and 4 can be attributed to cus $Mo^{\phi+}$ sites ($2 < \phi < 4$), as is reported in most of the studies on $MoS_2$ catalysts. The double peak with the second feature at 2090 $cm^{-1}$ (Mo–B sites), which evolves upon $H_2$ treatment (Fig. 5b) and thiophene HDS (Fig. 4d), is only reported in few other studies by Maugé et al. [21–23]. They attribute this second feature to Mo sites situated on the Mo-edges, same as the Mo–A sites, but with a lower coordination number. Our results agree with this interpretation. The shoulders at 2066 $cm^{-1}$ (Mo–C sites), visible in Figs. 2 and 4, can be attributed to highly unsaturated Mo atoms located either on the sulfur edges [23] or the corners of the $MoS_2$ slabs [26]. Travert et al. [21] reported a minor feature at high wave number, viz., at 2130 $cm^{-1}$, after $H_2S$ exposure of a $MoS_2$ catalyst, however, this feature was not observed in the spectra of the present study. We expect that fully sulfur-coordinated $Mo^{4+}$ sites are favored under sulfiding conditions, but that CO can hardly probe these Mo–S sites.

The different CO adsorption sites can be described using the model shown in Fig. 1. Starting with a completely sulfided $MoS_2$ catalyst, all edge sites are fully coordinated with sulfur. CO will not be able to adsorb on these Mo–S sites (vide supra). Upon removal of sulfur atoms, vacant Mo sites with a high sulfur coordination number are formed initially (Mo–A), which are gradually transformed into vacant Mo sites with a lower coordination number (Mo–B). This is in agreement with the CO spectra of the Mo catalyst: mainly Mo–A sites (2105 $cm^{-1}$) are present directly after sulfiding (Fig. 5a). Mo–A sites gradually disappear after $H_2$ and thiophene exposure, while Mo–B sites (2090 $cm^{-1}$) appear and become the most prominent feature (Fig. 5b and c). Remarkably, the Mo–C sites are stable during the reaction-resulfidation cycle (Fig. 5d), in contrast to the Mo–A and Mo–B edge sites, which are probably covered by coke (see Section 4.3).

#### 4.2.2. Promoted catalysts

The promoted catalysts show various spectral features not observed in the unpromoted ones, which can therefore be attributed to CO adsorption on the NiMoS phase. New bands are observed at 2118 $cm^{-1}$ (NiMo–S) and 2088 $cm^{-1}$ (NiMo–A) in the IR spectra of the NiMo catalysts treated for 0.5 h in $H_2$ (Fig. 3). According to Table 2, these bands can be attributed to $Ni^{\delta+}$ sites ($0 < \delta < 2$). However, there is also the possibility that CO is adsorbed on a Mo site interacting with the promoter, as suggested by Lélias et

al. for the CoMoS phase [20]. Therefore, we have labeled these sites "NiMo". The strong intensity of the 2118 $cm^{-1}$ band upon sulfiding indicates that these NiMo–S sites are favored under sulfiding conditions and probably highly sulfur coordinated. Still, the significant CO adsorption suggests that the sulfur coordination is not 100%, in contrast to the analogous Mo–S sites, yet maximal under the sulfiding conditions applied. Further reductive treatment or exposure to reaction conditions (Figs. 6 and 7) results in a very broad band around 2077 $cm^{-1}$ (NiMo–B sites), also reported by Angulo et al. [24]. There is a parallel between the IR spectra of the promoted and unpromoted catalysts. The absorption maximum shifts from 2088 to 2077 $cm^{-1}$ upon prolonged reductive treatment (see the sequence of figures: Figs. 4b–d and 7a–c). Hence, these positions in the spectrum (2088 and 2077 $cm^{-1}$) can be attributed to cus $Ni^{\delta+}$ sites with high (NiMo–A) and low (NiMo–B) coordination number, similar to the Mo–A and Mo–B type sites. The strong peak broadening around 2050 $cm^{-1}$ (Fig. 3) suggests the presence of highly cus promoted sites (NiMo–C), analogous to the Mo–C sites.

### 4.3. Structure–activity relations

All four catalysts lose a significant part of their initial activity during the first 4 h on stream in the gas phase HDS of thiophene (Fig. 9). It was concluded previously [10] that the loss of structural sulfur from the active phase during the reaction was the main reason for the observed deactivation under these conditions. The present in situ spectroscopic results give additional evidence for this conclusion. Clearly, the CO IR spectrum of the Mo catalyst after 2 h of thiophene HDS (Fig. 4c) has the same shape as the spectrum after 4 h of $H_2$ exposure (Fig. 5b). Also, the spectra of the NiMo catalyst after 2 or 4 h of thiophene HDS (Fig. 4c and d) show a close resemblance to the spectrum after 4 h exposure to $H_2$ (Fig. 6b). Upon $H_2$ treatment, the active phase of both Mo and NiMo catalysts transforms from a fully sulfided or coordinatively saturated state (Fig. 5a, 6a and 7a) to an unsaturated or desulfided state (Figs. 5b, 6b and 7b). This "desulfidation process" is characterized by the increased number of CO adsorption sites and by the higher degree of unsaturation, indicated by the peak shift toward lower wavenumbers (see Sections 4.2 and 4.3). A similar process occurs during thiophene HDS (Fig. 4c).

It was shown earlier [10] that the activity of a Type I NiMo catalyst could be fully recovered by a resulfidation treatment after the thiophene HDS reaction. The IR spectra of the NiMo catalyst (Figs. 6d,e and 7d) confirm that the active phase is restored to its initial (sulfided) state by a resulfiding treatment. However, the behavior is different for the Mo catalyst: the spectra of the freshly sulfided (Fig. 5a) and resulfided catalysts look similar (Fig. 5d), but apparently a fraction of the CO adsorption sites is permanently lost. This agrees with the observation that only a part of the activity of a comparable Mo catalyst could be recovered upon resulfidation [10]. The irreversible loss of sites could be due to coke deposition, as was already concluded by Elst et al. [25]. Indeed, carbonaceous species are still present on the Mo catalyst after resulfidation (Fig. 5d). However, also the NiMo catalysts exhibit similar bands in the coke region of their IR spectra (Figs. 6d,e and 7d) without the loss of adsorption sites. This confirms that NiMo catalysts are able to suppress coke deposition on the active sites, whereas coke (partially) blocks the active phase in the case of Mo [10]. Furthermore, the reversibility of the spectra for the NiMo catalysts shows that the catalyst does not undergo dramatic structural changes, like sintering or segregation of the promoter, during the treatments applied.

#### 4.3.1. Thiophene HDS active sites

It is generally accepted that vacant sites on the edges of the active phase are required for the removal of sulfur from thiophenic molecules [1]. Therefore, one would expect that catalysts with more vacant sites exhibit a higher HDS activity. However, our results show the opposite trend: the fully sulfided catalysts have the highest thiophene HDS activity (Fig. 9) but the lowest number of cus sites (Fig. 4a). Some researchers propose that the rate-determining step in the gas phase HDS of thiophene is the (partial) hydrogenation of the thiophenic ring [11,29,30]. Others suggest that vacant sites are not required for this reaction step: simulations by Smit and Johnson [12] and experimental observations by Lauritsen et al. [11] indicate that the hydrogenation may be catalyzed by a fully sulfided $MoS_2$ system. Both publications state that thiophene interacts with the catalyst through S–S bonds. Lauritsen et al. suggest a second interaction between the p-electrons of the thiophenic ring and the "metallic brim" formed by S atoms on the $MoS_2$ basal plane [11]. Our results cannot substantiate these theories. Nevertheless, it is concluded that the gas phase thiophene HDS activity does not correlate with the number of vacant sites on the catalyst, but rather with the number of sulfur-covered sites. These sites must be involved in the rate-determining step of the thiophene HDS reaction, probably the hydrogenation step.

#### 4.3.2. Dibenzothiophene HDS active sites

The case of liquid phase dibenzothiophene HDS is different as compared to gas phase thiophene HDS. The CO adsorption spectrum of the NiMo catalyst after DBT exposure (Fig. 8) is similar to that of the freshly sulfided one (Fig. 4a). Apparently, the "desulfidation process" does not occur in the liquid phase under the conditions applied. Subsequent treatments in $H_2$ and $H_2S$ yield the expected IR patterns, which indicates that the transfer from the autoclave to the IRIS setup did not irreversibly affect the sample, e.g. by oxidation.

The liquid phase activity measurements (Fig. 10) show the expected reaction products, where DBT is either directly desulfurized to biphenyl (DDS route) or prehydrogenated and desulfurized to (HYD route) cyclohexylbenzene [14]. Hence, the observed CHB/BPh ratio (Fig. 11) is a measure for the HYD/DDS selectivity. The catalyst pretreated in $H_2$ shows a lower HYD selectivity than the standard sulfided catalyst. The total time needed for DBT conversion remains the same, which means that the DDS rate increases while the HYD rate decreases, keeping the total activity equal. This implies that DDS sites are formed at the expense of HYD sites. The results presented before (Section 4.2.2) show that the $H_2$ pretreatment results in an increase in the number of vacant sites. This indicates that the rate-determining step in DDS route is catalyzed by vacant sites, whereas the rate-determining step in the HYD route is catalyzed by sulfided species on the catalyst, similar to the thiophene reaction. The results presented in this study clearly demonstrate the power of combining IR spectroscopy of adsorbed CO and HDS activity testing, showing that structure–activity relations can be identified and substantiated for this type of catalysts.

## 5. Conclusions

IR analysis of adsorbed CO proved to be an excellent technique to study the active phase of HDS catalysts. The differences between Mo and NiMo based catalysts were clearly visible using this method, probing both the unpromoted $MoS_2$ and the NiMoS phase. The use of NTA as chelating agent had a marked effect on the active phase of the NiMo catalyst: the NTA based catalyst (Type II) had a fully promoted edge structure, whereas the Type I catalyst exhibited both promoted and unpromoted edge sites. This confirms that the NTA complex improves the decoration of the $MoS_2$ slabs by the promoter atoms.

The present results show that the active phase of $MoS_2$ based catalysts has a dynamic character. The sulfur coordination strongly depends on the pretreatment or reaction conditions applied and this behavior is reversible. The IR analysis confirmed that the num-

ber of vacant sites on the catalyst and/or the degree of coordinative unsaturation of these sites increased during gas phase thiophene HDS, causing deactivation. In the case of NiMo, the active phase could be fully restored to its initial state by resulfiding, whereas some of the active sites on the Mo catalysts were irreversibly lost, possibly by coke deposits. The observed thiophene HDS conversion, as well as the conversion of dibenzothiophene to cyclohexylbenzene (HYD), decreased with the number of vacant sites present on the catalyst surface, whereas the conversion of dibenzothiophene to biphenyl (DDS) increased. The combined information from the IR characterization and activity tests showed that the rate-determining steps of the thiophene HDS reaction and the dibenzothiophene HYD pathway are catalyzed by sulfided species on the active phase and that the rate-determining step of the DDS pathway is catalyzed by vacant sites.

## Acknowledgements

Mr. S. Driessen is gratefully acknowledged for experimental support. Albemarle Catalysts and NWO are gratefully acknowledged for their financial support.

## References

[1] H. Topsøe, B.S. Clausen, F.E. Massoth, Hydrotreating Catalysis, Springer, Berlin, 1996.
[2] S. Helveg, J.V. Lauritsen, E. Laegsgaard, I. Stensgaard, J.K. Norskov, B.S. Clausen, H. Topsoe, F. Besenbacher, Phys. Rev. Lett. 84 (2000) 951–954.
[3] J.V. Lauritsen, S. Helveg, E. Lægsgaard, I. Stensgaard, B.S. Clausen, H. Topsøe, F. Besenbacher, J. Catal. 197 (2001) 1–5.
[4] L.S. Byskov, M. Bollinger, J.K. Norskov, B.S. Clausen, H. Topsoe, J. Mol. Catal. A: Chem. 163 (2000) 117–122.
[5] H. Schweiger, P. Raybaud, G. Kresse, H. Toulhoat, J. Catal. 207 (2002) 76–87.
[6] A. Travert, H. Nakamura, R.A. van Santen, S. Cristol, J.F. Paul, E. Payen, J. Am. Chem. Soc. 124 (2002) 7084–7095.
[7] P. Raybaud, Appl. Catal. A: Gen. 322 (2007) 76–91.
[8] M. Sun, J. Adjaye, A.E. Nelson, Appl. Catal. A: Gen. 263 (2004) 131–143.
[9] S. Eijsbouts, Appl. Catal. 158 (1997) 53–94.
[10] B.M. Vogelaar, P. Steiner, Th.F. van der Zijden, A.D. van Langeveld, S. Eijsbouts, J.A. Moulijn, Appl. Catal. A: Gen. 318 (2007) 28–36.
[11] J.V. Lauritsen, M. Nyberg, J.K. Norskov, B.S. Clausen, H. Topsøe, E. Laegsgaard, F. Besenbacher, J. Catal. 224 (2004) 94–106.
[12] T.S. Smit, K.H. Johnson, J. Mol. Catal. 91 (1994) 207–222.
[13] D.H. Broderick, B.C. Gates, AIChE J. 27 (1981) 663–673.
[14] B.M. Vogelaar, N. Kagami, A.D. van Langeveld, S. Eijsbouts, J.A. Moulijn, Prep. Am. Chem. Soc.: Div. Fuel Chem. 48 (2003) 548–549.
[15] N. Sheppard, C. de la Cruz, Catal. Today 70 (2001) 3–13.
[16] A. Fohlisch, M. Nyberg, P. Bennich, L. Triguero, J. Hasselstrom, O. Karis, L.G.M. Pettersson, A. Nilsson, J. Chem. Phys. 112 (2000) 1946–1958.
[17] L.P. Nielsen, L. Ibsen, S.V. Christensen, B.S. Clausen, J. Mol. Catal. A: Chem. 162 (2000) 367–371.
[18] E.J.M. Hensen, P.J. Kooyman, Y. van der Meer, A.M. van der Kraan, V.H.J. de Beer, J.A.R. van Veen, R.A. van Santen, J. Catal. 199 (2001) 224–235.
[19] R. Cattaneo, F. Rota, R. Prins, J. Catal. 199 (2001) 318–327.
[20] M.A. Lélias, J. van Gestel, F. Maugé, J.A.R. van Veen, Catal. Today 130 (2008) 109–116.
[21] A. Travert, C. Dujardin, F. Maugé, S. Cristol, J.F. Paul, E. Payen, D. Bougeard, Catal. Today 70 (2001) 255–269.
[22] J. van Gestel, C. Dujardin, F. Maugé, J.C. Duchet, J. Catal. 202 (2001) 78–88.
[23] C. Dujardin, M.A. Lélias, J. van Gestel, A. Travert, J.C. Duchet, F. Maugé, Appl. Catal. A: Gen. 322 (2007) 46–57.
[24] M. Angulo, F. Maugé, J.C. Duchet, J.C. Lavalley, Bull. Soc. Chim. Belg. 96 (1987) 925–929.
[25] L.P.A.F. Elst, S. Eijsbouts, A.D. van Langeveld, J.A. Moulijn, J. Catal. 196 (2000) 95–103.
[26] B. Müller, A.D. van Langeveld, J.A. Moulijn, H. Knözinger, J. Phys. Chem. 97 (1993) 9028–9033.
[27] Z. Wu, F. Sun, W. Wu, Z. Feng, C. Liang, Z. Wei, C. Li, J. Catal. 222 (2004) 41–52.
[28] J.B. Peri, J. Catal. 86 (1984) 84–94.
[29] P. Raybaud, J. Hafner, G. Kresse, H. Toulhoat, Stud. Surf. Sci. Catal. 127 (1999) 309–317.
[30] X.Q. Yao, Y.W. Li, H. Jiao, J. Mol. Struct.: Theochem. 726 (2005) 81–92.